

Magnetite Nanocrystals: Nonaqueous Synthesis, Characterization, and Solubility[†]

Nicola Pinna,^{*,‡} Stephanie Grancharov,[§] Pablo Beato,^{||} Pierre Bonville,[⊥]
Markus Antonietti,[§] and Markus Niederberger[§]

Institut für Anorganische Chemie, Martin-Luther-Universität Halle-Wittenberg, Kurt-Mothes-Strasse 2, 06120 Halle (Saale), Germany, Max-Planck-Institute of Colloids and Interfaces, Research Campus Golm, 14424 Potsdam, Germany, Department of Inorganic Chemistry, Fritz-Haber-Institute of the Max-Planck-Society, Faradayweg 4-6, D-14195 Berlin, Germany, and CEA, CE Saclay, DSM/DRECAM/SPEC, 91191 Gif-Sur-Yvette, France

Received January 11, 2005. Revised Manuscript Received March 30, 2005

A novel nonaqueous route has been applied for the preparation of nanocrystalline magnetite. In a simple one-pot reaction process, iron(III) acetylacetonate was dissolved in benzyl alcohol and treated in an autoclave between 175 and 200 °C. This approach leads to monocrystalline magnetite particles with sizes ranging from 12 to 25 nm, as evidenced by X-ray analysis, HRTEM, and Raman and Mössbauer spectroscopy. The isolated particles can be redispersed either in polar or nonpolar solvents by coating them just after synthesis with undecanoic acid or dopamine. Simple sedimentation after redispersion in hexane can be used to lower the polydispersity of the sample.

1. Introduction

It can be safely stated that the synthesis of controlled-size magnetic particles is of high scientific and technological interest.^{1,2} As previously described in multiple publications, they are useful for many applications; in particular for magnetic recording or biomedical applications.^{3–6}

Iron oxide nanoparticles are usually synthesized in aqueous solutions^{7–9} via coprecipitation of Fe(II) and Fe(III) ions by a base. During these reactions several parameters have to be controlled carefully, including pH, method of mixing, temperature, the nature and concentration of the anions, etc. Other synthesis methods such as polyol-mediated sol–gel¹⁰ and sonochemical¹¹ were also proposed. To overcome the limitations introduced by aqueous precipitation reactions several groups have developed nonaqueous approaches for the production of metal oxide nanoparticles and in particular

iron oxide. For example, the reaction of FeCup₃ with trioctylamine at 300 °C leads to 6–7 nm maghemite nanocrystals,¹² and the reaction of Fe(acac)₃ in a mixture of four solvents and ligands, namely phenyl ether, 1,2-hexadecanediol, oleic acid, and oleylamine, leads to 4-nm magnetite nanoparticles.¹³ By decomposition of Fe(CO)₅ in octyl ether and oleic acid or lauric acid and subsequent oxidation, high-quality maghemite nanoparticles with size ranging from 4 to 16 nm have been produced.¹⁴ Finally, the reaction of Fe(acac)₃ with 2-pyrrolidone leads to 5-nm magnetite particles.¹⁵ These results showed the effectiveness of the nonaqueous routes for the production of well-calibrated iron oxide nanoparticles. However, these approaches are not exempt of drawbacks; in fact, use of massive amounts of surfactants like oleylamine, oleic acid, trioctylamine, etc., is of environmental concern, and, furthermore, the obtained particles are coated by large quantities of surfactants. This seriously limits biomedical applications.

In this work we show that such drawbacks can be overcome by using only benzyl alcohol (BA) as solvent and ligand at the same time, instead of the mixtures of solvents and ligands commonly used. In fact BA is an environmentally friendly solvent and commonly used in the food industry. Furthermore BA has already proven to be a suitable “soft” solvent/ligand for the synthesis of several binary metal oxide nanoparticles, perovskites, and hybrid materials.^{16–24}

[†] Nicola Pinna would like to dedicate this article to Prof. Dr. J. Urban and Klaus Weiss on the occasion of their retirement for their contributions in the studies of nanoparticles.

* Corresponding author. E-mail: nicola.pinna@chemie.uni-halle.de. Tel: 49 345 55 25870. Fax: 49 345 55 27343.

[‡] Martin-Luther-Universität Halle-Wittenberg.

[§] Max-Planck-Institute of Colloids and Interfaces.

^{||} Fritz-Haber-Institute of the Max-Planck-Society.

[⊥] CEA, CE Saclay, DSM/DRECAM/SPEC.

- (1) Leslie-Pelecky, D. L.; Rieke, R. D. *Chem. Mater.* **1996**, *8*, 1770.
- (2) Raj, K.; Moskowitz, R. *J. Magn. Magn. Mater.* **1990**, *85*, 233.
- (3) Awschalom, D. D.; Di Vincenzo, D. P. *Phys. Today* **1995**, *4*, 43.
- (4) Spiliotis, D. E. *J. Magn. Magn. Mater.* **1999**, *193*, 29.
- (5) Levy, L.; Sahoo, Y.; Kim, K.-S.; Bergey, E. J.; Prasad, P. N. *Chem. Mater.* **2002**, *14*, 3715.
- (6) Berry, C. C.; Curtis, A. S. G. *J. Phys. D: Appl. Phys.* **2003**, *36*, R198.
- (7) Sugimoto, T.; Matijevic, E.; *J. Colloid Interface Sci.* **1980**, *74*, 227.
- (8) Kang, Y. S.; Risbud, S.; Rabolt, J. F.; Stroeve, P. *Chem. Mater.* **1996**, *8*, 2209.
- (9) Fried, T.; Shemer, G.; Markovich, G. *Adv. Mater.* **2001**, *13*, 1158.
- (10) Feldmann, C.; Jungk, H.-O. *Angew. Chem., Int. Ed.* **2001**, *40*, 359.
- (11) Vijaya Kumar, R.; Koltypin, Yu.; Cohen, Y. S.; Cohen, Y.; Aurbach, D.; Palchik, O.; Felner, I.; Gedanken, A. *J. Mater. Chem.* **2000**, *10*, 1125.

- (12) Rockenberger, J.; Scher, E. C.; Alivisatos, A. P. *J. Am. Chem. Soc.* **1999**, *121*, 11595.
- (13) Sun, S.; Zeng, H. *J. Am. Chem. Soc.* **2002**, *124*, 8204.
- (14) Hyeon, T.; Lee, S. S.; Park, J.; Chung, Y.; Na, H. B. *J. Am. Chem. Soc.* **2001**, *123*, 12798.
- (15) Li, Z.; Chen, H.; Bao, H.; Gao, M. *Chem. Mater.* **2004**, *16*, 1391.
- (16) Niederberger, M.; Bartl, M. H.; Stucky, G. D. *Chem. Mater.* **2002**, *14*, 4364.
- (17) Niederberger, M.; Bartl, M. H.; Stucky, G. D. *J. Am. Chem. Soc.* **2002**, *124*, 13642.

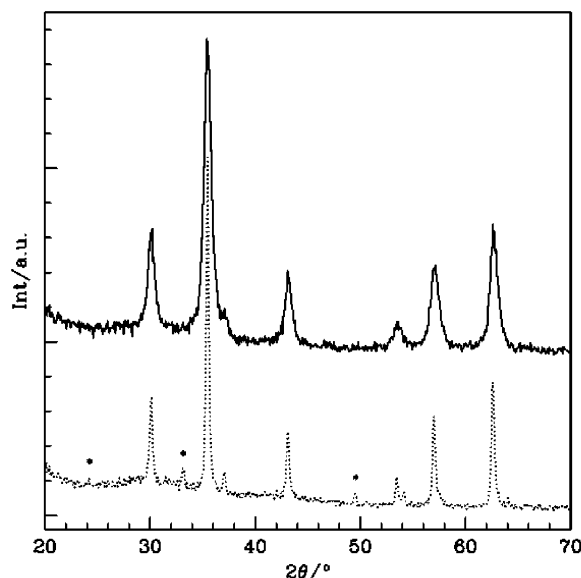


Figure 1. XRD patterns of the magnetite particles synthesized at 175 °C (solid line) and 200 °C (dotted line). The positions of the peaks of the hematite structure are marked with asterisks (*).

Here we report the one-pot reaction between benzyl alcohol and iron(III) acetylacetonate for the formation of high-purity magnetite nanocrystals. It is the special advantage of this technique that the particles could be easily coated after synthesis with minimal amounts of ligands and redispersed either in polar or nonpolar solvents.

2. Results and Discussion

2.1. Structural Characterization. Iron(III) acetylacetonate in benzyl alcohol provides a versatile reaction system for the nonaqueous preparation of iron oxide nanoparticles. The synthetic procedure results directly in the formation of a black powder.

All samples were investigated by X-ray powder diffraction (XRD). When the synthesis temperature was 175 °C the pattern presented broad peaks (Figure 1 solid line) characteristic of the structure of magnetite (Fe_3O_4) at the nanometer scale (JCPDS 19-629). Estimation of the particle size from the peak broadening gives a mean value of 10.5 nm. The powder diffraction pattern of particles synthesized at a higher temperature (200 °C) presents sharper peaks (Figure 1 dotted line). As expected the average size estimated from the peak broadening gives a larger value of 29 nm. In this case three additional low-intensity peaks (marked with asterisks) are present that do not belong to the magnetite structure. They can be attributed to a low amount of hematite ($\alpha\text{-Fe}_2\text{O}_3$).

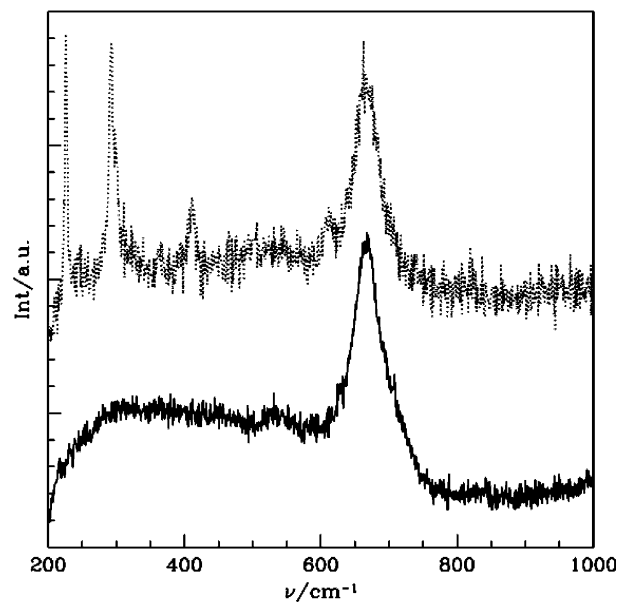


Figure 2. Raman spectra of the magnetite particles synthesized at 175 °C (solid line) and 200 °C (dotted line).

The XRD patterns of magnetite (Fe_3O_4) and maghemite ($\gamma\text{-Fe}_2\text{O}_3$) are very similar. The main difference consists of a few low-intensity diffractions (<5%) which are only present for the maghemite structure. These diffraction lines are not present in the patterns presented in Figure 1. Nevertheless, since they are only low-intensity peaks one cannot exclude the presence of maghemite in the samples. The technique used to discriminate between the two structures often consists of the oxidation of the material at higher temperatures, to observe whether the transformation from magnetite to maghemite takes place. This method, even if widely employed, is not suitable for nanoparticles, because the particle size increases during the thermal treatment. Therefore, the fact that the low intensity peaks become visible in the XRD pattern does not prove that the transition from magnetite to maghemite took place; it could simply be due to an increase of the particle size.

However, the different structural phases of iron oxides can be easily distinguished by Raman spectroscopy.²⁵ Magnetite has a main band centered at 668 cm^{-1} (A_{1g})²⁶ whereas maghemite ($\gamma\text{-Fe}_2\text{O}_3$) shows broad structures around 700, 500, and 350 cm^{-1} .²⁷ Figure 2 illustrates the Raman spectra measured for the two particle sizes.

The smaller particles synthesized at 175 °C (Figure 2 solid line) exhibit a main band centered at 667 cm^{-1} , which is in good agreement with the positions found in the literature for magnetite. Under heat treatment magnetite is known to transform at around 200 °C to maghemite which is then transformed at around 400 °C to hematite ($\alpha\text{-Fe}_2\text{O}_3$). Similar structural transformations have been observed under laser irradiation of magnetite powder samples.²⁸ Shebanova et al. stated that the laser-induced transformations occurred directly

- (18) Niederberger, M.; Garnweitner, G.; Krumeich, F.; Nesper, R.; Cölfen, H.; Antonietti, M. *Chem. Mater.* **2004**, *16*, 1202.
- (19) Pinna, N.; Antonietti, M.; Niederberger, M. *Colloids Surf., A* **2004**, *250*, 211.
- (20) Pinna, N.; Garnweitner, G.; Antonietti, M.; Niederberger, M. *Adv. Mater.* **2004**, *16*, 2196.
- (21) Pinna, N.; Garnweitner, G.; Beato, P.; Niederberger, M.; Antonietti, M. *Small* **2005**, *1*, 112.
- (22) Niederberger, M.; Pinna, N.; Polleux, J.; Antonietti, M. *Angew. Chem., Int. Ed.* **2004**, *43*, 2270.
- (23) Niederberger, M.; Garnweitner, G.; Pinna, N.; Antonietti, M. *J. Am. Chem. Soc.* **2004**, *126*, 9120.
- (24) Pinna, N.; Neri, G.; Antonietti, M.; Niederberger, M. *Angew. Chem., Int. Ed.* **2004**, *43*, 4345.

- (25) Cornell, R. M.; Schwertmann, U. *The Iron Oxides*; VCH: New York, 1996; p 135.
- (26) Shebanova, O. N.; Lazor, P. *J. Solid State Chem.* **2003**, *174*, 424.
- (27) De Faria, D. L. A.; Venancio Silva, S.; De Oliveira, M. T. *J. Raman Spectrosc.* **1997**, *28*, 873.
- (28) Shebanova, O. N.; Lazor, P. *J. Raman Spectrosc.* **2003**, *34*, 845.

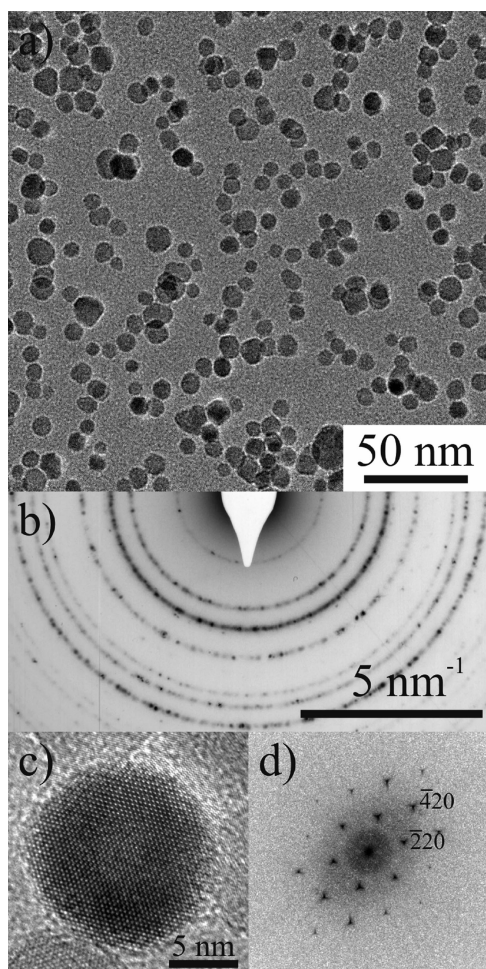


Figure 3. TEM overview of the particles synthesized at 175 °C (a), electron diffraction of a large zone (b), HRTEM of a unique single-crystal particle (c) and its power spectrum (d).

from magnetite to hematite when coarse-grained ($d > 1 \mu\text{m}$) magnetite powder was used, but they observed intermediate formation of maghemite if fine-grained ($d = 0.3\text{--}1 \mu\text{m}$) magnetite powder was used. In our Raman experiments, under laser irradiation, we observed the appearance of two broad features around 700 and 500 cm^{-1} , which can be attributed to maghemite. After a longer irradiation time bands at 220, 284, 300, 400, 491, and 600 cm^{-1} confirmed the transformation to hematite.

The pattern of the larger particles synthesized at 200 °C (Figure 2 dotted line) shows the same main feature at 667 cm^{-1} characteristic of magnetite. In addition, it also exhibits the bands characteristic of the hematite structure. Although these bands are quite intense, the total amount of hematite in the sample is supposed to be well below 5%, as the cross section of these Raman bands of hematite is much larger than that of magnetite. This point will be confirmed by the ^{57}Fe Mössbauer spectra (see below).

Figure 3a shows a transmission electron microscopy (TEM) overview image of an assembly of particles synthesized at 175 °C. It shows rather uniform sizes and shapes, even though no size selection was applied to the as-synthesized particles, which is what is commonly done by centrifugation to eliminate the larger particles that could not be stabilized by the solvent.²⁹ This technique leads to a lower polydispersity but also to a lower yield. The overview TEM

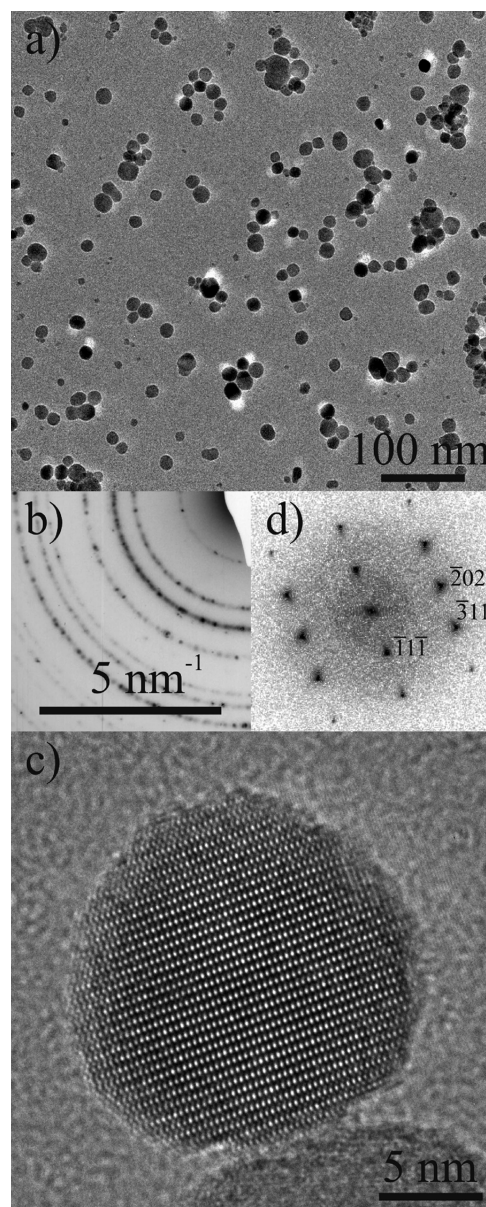


Figure 4. TEM overview of the particles synthesized at 200 °C (a), electron diffraction of a large zone (b), HRTEM of a unique single-crystal particle (c) and its power spectrum (d).

image (Figure 3a) is characteristic of the whole sample ($\sim 500 \text{ mg}$). Electron diffraction measured from a large zone (Figure 3b) presents rings that can be indexed to the magnetite structure. The reflections characteristic of maghemite are not observed. High-resolution TEM (Figure 3c) demonstrates the high crystallinity of a typical particle of 12-nm diameter. Each particle is a single crystal and does not have any structural defaults. The square of the Fourier transform of the HRTEM image (power spectrum, PS) shows the reflections characteristic of a single-crystal oriented along the $[111]$ zone axis (Figure 3d).

An overview image of the particles synthesized at 200 °C shows that these particles have larger sizes and a slightly larger polydispersity (Figure 4a). The average size determined by TEM is around 20–25 nm. The electron diffraction

(29) Sun, S.; Zeng, H.; Robinson, D. B.; Raoux, S.; Rice, P. M.; Wang, S. X.; Li, G. *J. Am. Chem. Soc.* **2003**, *126*, 273.

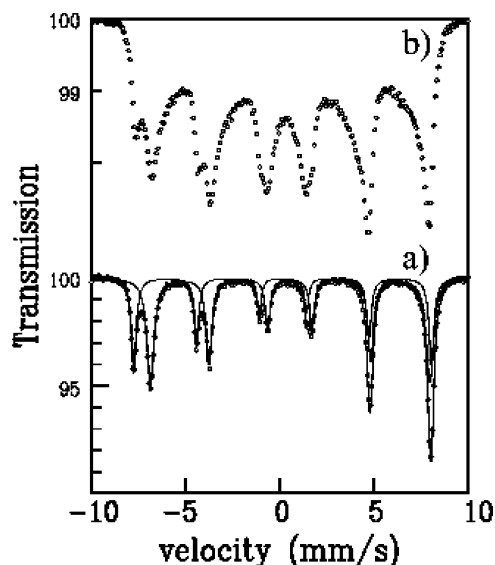


Figure 5. ^{57}Fe Mössbauer spectra at room temperature in the two samples synthesized at 200 °C (a) and at 175 °C (b). The solid line in (a) is a fit by two magnetic hyperfine sextets.

is, also in this case, characteristic of magnetite (Figure 4b). HRTEM of an 18-nm particle shows well-defined lattice planes with perfect crystallinity (Figure 4c). The sharp reflections of its PS can be unambiguously attributed to the magnetite structure for a particle oriented along the [121] direction (Figure 4d).

Structural characterization gives a clear idea of the phase and the purity of the samples. For particles synthesized at 175 °C only magnetite was found; however, in the case of the synthesis at higher temperatures a small quantity of hematite was found in addition to magnetite. To confirm these results, Mössbauer spectra on the isotope ^{57}Fe were performed at room temperature on the two samples (Figure 5).

The obtained spectra confirm that both samples are made of magnetite. The spectrum in the larger particles (Figure 5a) is typical of “bulk” magnetite and can be fitted with two magnetic hyperfine sextets.³⁰ Due to the good statistics of the spectrum, the amount of hematite in the sample can be said to be lower than 1.5%. The spectrum in the smaller particles (Figure 5b) shows lines at the same positions as in the “bulk” spectrum, but two main differences are visible: (i) the lines present a distortion with respect to the standard Lorentzian shape, pointing to the presence of an asymmetrical distribution of hyperfine fields; and (ii) there is a broad absorption in the center of the spectrum, which points to the presence of fluctuation broadened spectral components.

Actually, both features are characteristic of small particles³¹ showing superparamagnetic fluctuations with frequencies below, but close to, the Mössbauer hyperfine Larmor frequency ($\nu_L \approx 50$ MHz for ^{57}Fe). However, no fit is shown for this spectrum due to the lack of a suitable model encompassing the spectral effects of superparamagnetic behavior. The comparison of the two spectra is in agreement with the mean size assignment from the TEM pictures:

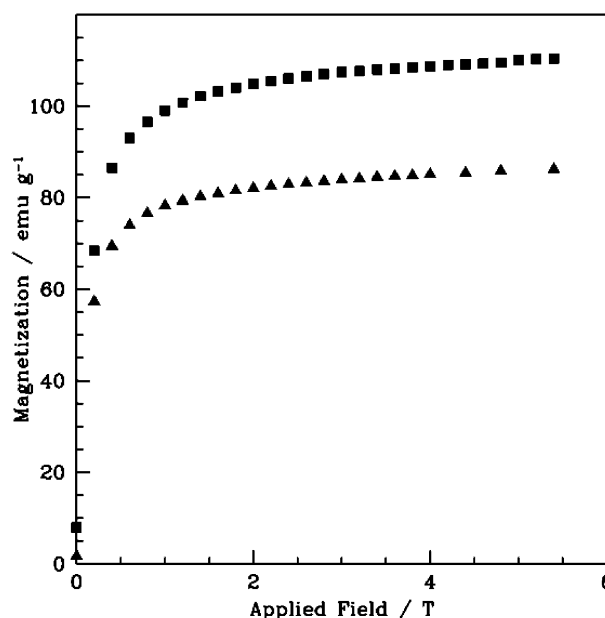


Figure 6. Magnetization curves at 5 K in the two samples synthesized at 200 °C (■) and at 175 °C (▲).

particles made at 200 °C must have diameters well above the superparamagnetic “blocking diameter” d_b for Mössbauer spectroscopy at room temperature, whereas particles made at 175 °C must present a fraction which has diameters close to or below d_b . An approximate expression for the blocking diameter at temperature T is³²

$$d_b = \left[\frac{6 k_B T}{\pi K} \ln \frac{\nu_0}{\nu_L} \right]^{1/3} \quad (1)$$

where K is the anisotropy constant of the material and ν_0 is an attempt frequency of the order of 10^{10} to 10^{11} s⁻¹. The blocking diameter deduced from the data must be lower than 25 nm (mean size of the larger particles), and close to 10 nm (mean size of the smaller particles). Expression 1 shows that a value $K = 5 \times 10^4$ J/m³ yields $d_b = 9$ nm, with the values of the anisotropy constant derived in ref 31 for nanometric Fe₃O₄ particles. This matches with the discussion above.

The saturation magnetization (M_S) was determined at 5 K for both samples by measuring magnetization curves (Figure 6). For an applied field of 5.4 T the magnetization was 86.2 emu/g for the smaller particles and 110.4 emu/g for the largest ones synthesized at 200 °C. Those large values are comparable to the one of the bulk magnetite (100 emu/g) proving that the nanocrystals synthesized by the benzyl alcohol route could lead to various applications.

In conclusion, structural characterization studies demonstrate that the nanoparticles synthesized from iron(III) acetylacetonate in benzyl alcohol are principally made of magnetite and show an extraordinarily high crystallinity (i.e., each particle studied by HRTEM presented a monocrystalline behavior). This is probably the reason their saturation magnetization is comparable to that of bulk magnetite.

2.2. Size Selection and Redispersion in Polar or Non-polar Solvents. The nanoparticles after synthesis can be

(30) Murad, E. *Iron in Soils and Clay Minerals*; D. Reidel Publishing Co.: Dordrecht, Holland, 1988.

(31) Mørup, S.; Topsøe, H.; Lipka, J. *J. Phys. (Paris)* **1976**, *37*, C6–287.

(32) Bean, C. P.; Livingston, J. D. *J. Appl. Phys.* **1959**, *30*, 120S.

extensively washed with solvent and isolated as a dry and clean powder. In this case no organic compounds were observed by Raman spectroscopy, suggesting that the amount of molecules adsorbed at the surface of the particles should be rather low. In addition, they can also be easily redispersed in water and hexane by coating with dopamine or undecanoic acid, respectively (see Experimental Section). After the particles are coated, it is possible to reduce the polydispersity of the sample by separation into species easy to disperse and a “precipitate” (it should be noted that this is not a permanent agglomerate), particularly for particles coated with undecanoic acid. Figure 7a shows a TEM image of particles synthesized at 175 °C (as for Figure 3a) after coating and redispersion in hexane. They are more homogeneous in size compared to the uncoated ones, and start to organize in a superlattice without any particular preparation. The average size decreases from 12 to 8 nm, due to the fact that the sediment was separated. When the particles are redispersed in water with the addition of dopamine after centrifugation, almost all particles go directly into solution. This is also confirmed by TEM (Figure 7b), which shows that the particles present a mean size and size distribution similar to that of the as-synthesized particles.

These findings were further confirmed by analytical ultracentrifugation (AUC) experiments which allow the direct determination of the size distribution of particles on the base of the whole sample set dispersed in the solvent (Figure 7c).^{18,33,34} The particles redispersed in hexane (dotted line) show a very narrow size distribution and an average diameter of 7.8 nm, in very good agreement with TEM studies. Redispersion in water does not decrease the polydispersity of the sample and the average size, which stays constant at 12.0 nm.

AUC therefore confirms the possibility to redisperse the magnetite nanoparticles easily in polar and nonpolar solvents by adding small amounts of stabilizing ligands, avoiding large losses of particles. Furthermore, the polydispersity could be considerably decreased by redispersion and fractionation in hexane.

Conclusion

Iron(III) acetylacetonate in benzyl alcohol provides a versatile reaction system for the nonaqueous preparation of magnetite nanoparticles. All the as-synthesized particles are crystalline, and the particle sizes can be easily tuned, either by the reaction temperature or by a postreaction fractionation.

The complete absence of any surfactant allows the synthesis of a high-purity material (just CHO contaminants, no ions, phosphorus, or sulfur) and permits the isolation of a clean nanocrystalline powder. The particles possess a very high degree of crystallinity as proved by HRTEM where every single particle is a single crystal without any structural defect.

The new approach is a simple, one-pot procedure using commercially available precursors and enables the cheap and

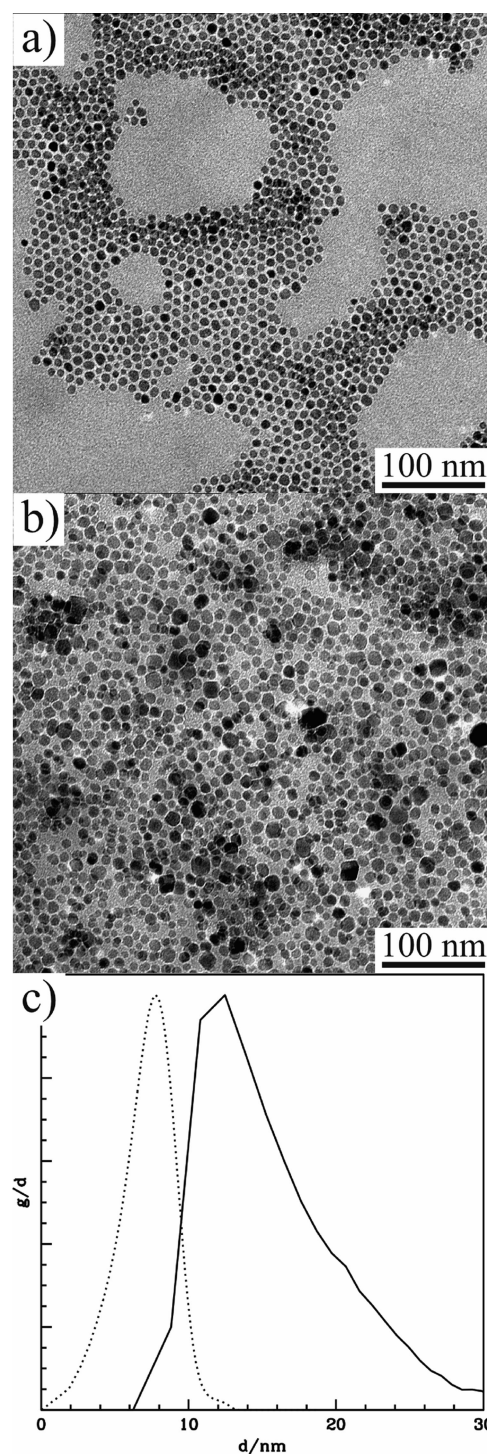


Figure 7. TEM overview of the particles synthesized at 175 °C redispersed in hexane (a), and water (b), analytical ultracentrifugation (AUC) of the particles in water (solid line) and hexane (dotted line). The lack of self-organization in (b) is due to the aqueous suspension, which does not allow for the organization of particles into a superlattice as in an organic solution.

multigram production of crystalline magnetite particles in the range between 8 and 25 nm.

Experimental Section

Synthesis. All the synthesis procedures were carried out in a glovebox (O_2 and $H_2O < 0.1$ ppm). In a typical synthesis of nanoparticles, 1.0 g of $Fe(acac)_3$ (2.81 mmol) was added to 20 mL of benzyl alcohol. The reaction mixture was transferred into a Teflon cup of 45-mL inner volume and slid into a steel autoclave which

(33) Cölfen, H.; Pauck, T. *Colloid Polym. Sci.* **1997**, 275, 175.

(34) Deshpande, A. S.; Pinna, N.; Beato, P.; Antonietti, M.; Niederberger, M. *Chem. Mater.* **2004**, 16, 2599.

was then carefully sealed. The autoclave was taken out of the glovebox and heated in a furnace at 175 or 200 °C for 2 days. The resulting dark suspensions were centrifuged, and the precipitates were thoroughly washed with ethanol and dichloromethane and subsequently dried in air at 60 °C.

For size-selection experiments just after synthesis the solution was poured into a centrifuge tube and placed in a centrifuge for 7 min at 5000 rpm. The solvent was then removed and discarded and 20 mL of hexane was added to the remaining precipitate. The solution was then placed in a stirring genie, sonicated, and slightly heated to 30 °C for 5 min. The solution was then broken into aliquots of 5 mL each.

A. For redispersion in hexane, 0.1 g of undecanoic acid was added, and the solution was sonicated for 5 min and then placed in a centrifuge for 7 min at 5000 rpm. The supernatant containing suspended particles was then poured off and saved, while any precipitates were discarded.

B. For redispersion in water, the hexane-containing solution was centrifuged and hexane was poured off from the sediment (there are no suspended particles). To the particle precipitate 0.1 g of dopamine and 1 mL of water was added. The solution was then placed in a stirring genie, sonicated in a heated environment (30 °C), and centrifuged for 7 min at 5000 rpm. Although some precipitates are present, most of the particles go into solution and exhibit prolonged colloidal shelf-stability.

Characterization. For transmission electron microscopy (TEM) studies one or more drops of the solution of the nanoparticles were deposited on the amorphous carbon film. The uncoated particles were dispersed in ethanol, whereas the ones coated with dopamine in water and the ones coated with undecanoic acid were dispersed in hexane. A Philips CM200 FEG microscope, 200 kV, equipped

with a field emission gun was used. The coefficient of spherical aberration was $C_s = 1.35$ mm. X-ray powder diffraction (XRD) patterns of all samples were measured in reflection mode (Cu K α radiation) on a Bruker D8 diffractometer equipped with a scintillation counter.

Raman spectra were measured in micro-Raman backscattering geometry. They were recorded using a HeNe laser (632.8 nm, Melles Griot, 17 mW) for excitation. The laser light was focused onto the sample using a 100 \times objective lens (Olympus) and the backscattered Raman lines were detected on a CCD camera (1024 \times 298 pixel), which was Peltier-cooled to 243 K to reduce thermal noise. The spectrometer was operated in the confocal mode setting the entrance slit to 200 μ m and the confocal hole to 400 μ m. A notch filter was applied to cut off the laser line and the Rayleigh scattering up to ca. 150 cm $^{-1}$.

The ^{57}Fe Mössbauer spectra were recorded using a commercial $^{57}\text{Co}:\text{Rh}$ radioactive source mounted on an electromagnetic drive with triangular velocity signal.

The particle size distribution was studied using a Beckman Optima XL-I analytical ultracentrifuge (Beckman Instruments, Palo Alto, CA) equipped with Rayleigh interference and UV absorption optics. The bulk density of magnetite was used to calibrate the size distributions curves.

Acknowledgment. We thank the Fritz-Haber-Institute and Prof. R. Schlögl for the use of the electron microscope and Klaus Weiss for his technical assistance. We thank Antje Völkel and Helmut Cölfen for the AUC measurements and helpful discussions. This project was partly supported by the German and American Fulbright Commission.

CM050060+